

Article

Photovoltaic Properties in Interpenetrating Heterojunction Organic Solar Cells Utilizing MoO₃ and ZnO Charge Transport Buffer Layers

Tetsuro Hori, Hiroki Moritou, Naoki Fukuoka, Junki Sakamoto, Akihiko Fujii * and Masanori Ozaki

Division of Electrical, Electronic and Information Engineering, Graduate School of Engineering, Osaka University, 2-1 Yamada-oka, Suita, Osaka 565-0871, Japan

* Author to whom correspondence should be addressed; E-Mail: afujii@opal.eei.eng.osaka-u.ac.jp; Tel.: +81-6-6879-7758; Fax: +81-6-6879-7774.

Received: 19 October 2010 / Accepted: 2 November 2010 / Published: 8 November 2010

Abstract: Organic thin-film solar cells with a conducting polymer (CP)/fullerene (C₆₀) interpenetrating heterojunction structure, fabricated by spin-coating a CP onto a C₆₀ deposit thin film, have been investigated and demonstrated to have high efficiency. The photovoltaic properties of solar cells with a structure of indium-tin-oxide/C₆₀/poly(3-hexylthiophene) (PAT6)/Au have been improved by the insertion of molybdenum trioxide (VI) (MoO₃) and zinc oxide charge transport buffer layers. The enhanced photovoltaic properties have been discussed, taking into consideration the ground-state charge transfer between PAT6 and MoO₃ by measurement of the differential absorption spectra and the suppressed contact resistance at the interface between the organic and buffer layers.

Keywords: organic solar cells; interpenetrating heterojunction; buffer layers; molybdenum trioxide; zinc oxide

1. Introduction

Since the discovery of photoluminescence quenching [1], photoinduced charge transfer [2], and photoconduction enhancement [3,4] in conducting polymers (CPs)-fullerene (C₆₀) systems, donor-acceptor type organic solar cells based on π -conjugated polymers have been investigated as next-generation solar cells. Two typical device structures, a layered structure [5] and a CP-C₆₀

composite structure [6], are mainly studied. However, a semi-layered structure with an interpenetrating interface has also been suggested as a candidate structure for obtaining high efficiency [7,8].

In the semi-layered structure, photoinduced charge transfer occurs efficiently because of the large interface area between donor and acceptor layers, and the generated electrons and holes can be transported efficiently to the electrodes. Previously, we developed a simple, yet effective method of fabricating such an interpenetrating interface, and reported an improvement in the photovoltaic conversion efficiency [9-14]. For the interpenetrating heterojunction type organic solar cell, we have reported buffer layer effects with the insertion of an appropriate metal oxide layer between the organic layer and the metal electrode, such as zinc oxide (ZnO) or molybdenum trioxide (VI) (MoO_3) [10,13,14]. We demonstrated the optimum film thicknesses of ZnO and MoO_3 layers, which act as electron and hole transport buffer layers, respectively. However, the studies about interpenetrating heterojunction type organic solar cells using both buffer layers and the mechanism of the photo conversion enhancement still remains to be carried out.

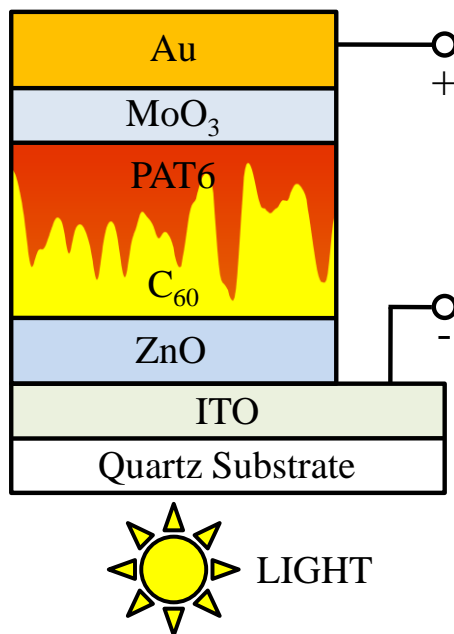
In this paper, we report on the improvement in the photovoltaic properties of the interpenetrating heterojunction solar cells upon the insertion of both MoO_3 and ZnO buffer layers and discuss about the enhanced photovoltaic properties.

2. Experimental

The solar cell structure of indium-tin-oxide (ITO)/ZnO/ C_{60} /poly(3-hexylthiophene) (PAT6)/ MoO_3 /Au, as shown in Figure 1, was fabricated in the following manner. A ZnO layer with a thickness of 50 nm [10] was sputtered onto ITO-coated quartz substrates. A C_{60} film with a thickness of approximately 130 nm was deposited by thermal evaporation onto the ZnO layer under 10^{-4} Pa at a substrate temperature of 150 °C [12]. The chloroform solution of PAT6, the concentration of which was 16.6 mg/mL, was spin-coated onto the C_{60} layer at 500 rpm for 5 sec and 1500 rpm for 30 sec. A MoO_3 layer and an Au electrode were fabricated by thermal evaporation through a shadow mask onto the PAT6 layer under a pressure of 10^{-4} Pa. The evaporation rates of MoO_3 and Au were approximately 0.3 Å/s and 1.0 Å/s and the thicknesses of the MoO_3 layer and Au electrode were 6 nm [13] and 70 nm, respectively. The active area of the solar cell was $1 \times 2 \text{ mm}^2$. In the cells, the ITO and Au electrodes collected electrons and holes, respectively.

The current-voltage characteristics were measured with a high-voltage-source measurement unit (Keithley 237) under AM1.5 (100 mW/cm^2) solar-illuminated conditions. From the current-voltage characteristics under AM1.5, the fill factor (FF) and energy conversion efficiency (η_e) were estimated using $\text{FF} = I_{\text{max}} V_{\text{max}} / I_{\text{sc}} V_{\text{oc}}$ and $\eta_e = I_{\text{sc}} V_{\text{oc}} \text{FF} / P_{\text{in}}$, where I_{max} and V_{max} are the current and voltage, respectively, for the maximum output power, I_{sc} is the short-circuit current density, V_{oc} is the open-circuit voltage, and P_{in} is the intensity of the incident light. The external quantum efficiency (EQE) spectra were measured under the short-circuit condition using an electrometer (Keithley 617S) and xenon lamp light passing through a monochromator as a light source. The current-voltage characteristics and EQE spectra were then measured in vacuum at room temperature. The EQE was estimated using $\text{EQE}(\%) = I_{\text{sc}} \times 124,000 / (\lambda(\text{nm}) \times P_{\text{in}})$, where λ is the wavelength of incident light. The UV-VIS-NIR absorbance spectra were measured using a spectrophotometer (Shimadzu UV-3150).

Figure 1. Schematic structure of interpenetrating heterojunction organic thin-film solar cell with metal oxide buffer layers.



3. Results and Discussion

The energy diagram of the solar cell with the ITO/ZnO/C₆₀/PAT6/MoO₃/Au structure is shown in Figure 2. According to the energy level of MoO₃, a negligible energy barrier for holes and a high energy barrier for electrons exist at the interface with PAT6. On the other hands, ZnO exhibits a negligible energy barrier for electrons and a high energy barrier for holes at the interface with C₆₀. In addition, since the buffer layers and adjacent electrodes form ohmic contacts, the internal electrical field intensity of the organic layers increases upon inserting buffer layers, therefore, it is expected that V_{oc} increases.

Figure 2. Schematic energy levels of ITO, ZnO, C₆₀, PAT6, MoO₃, and Au.

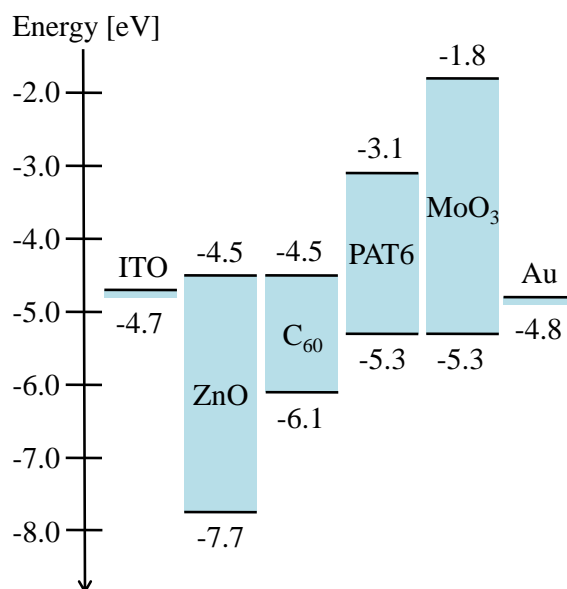
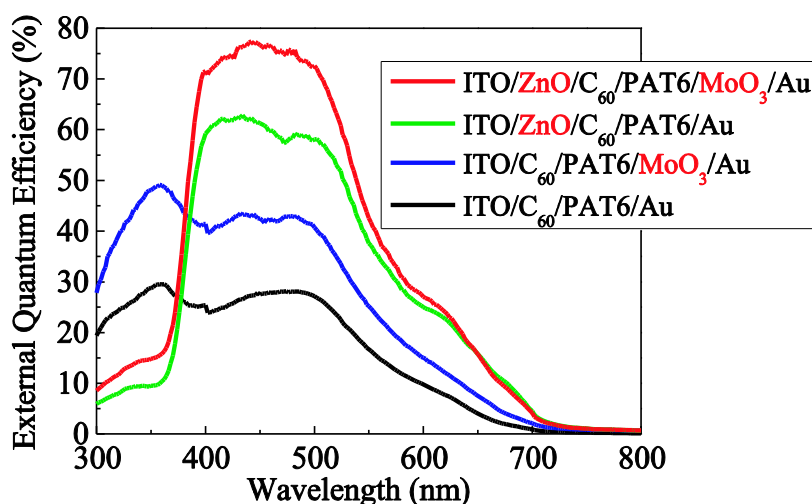


Figure 3 shows the EQE spectra of the solar cells with no buffer layer, the MoO₃ hole buffer layer, the ZnO electron buffer layer, and both buffer layers. The EQE of the solar cell with the MoO₃ hole buffer layer was about 40%, and that with the ZnO electron buffer layer was about 60% in the visible region. The EQE of the solar cell with the ZnO buffer layer decreased in the UV region, because the ZnO layer absorbs UV light and plays the role of a light filter. The EQE of the solar cell with both buffer layers increased further and exceeded 75%.

Figure 3. EQE spectra of the solar cells with no buffer layer, the MoO₃ buffer layer (6 nm), the ZnO buffer layer (50 nm), and the MoO₃ and ZnO buffer layers (6 nm and 50 nm, respectively).



The current-voltage characteristics of the same solar cells under AM1.5 (100 mW/cm²) solar-illuminated conditions are shown in Figure 4, and each performance parameter is summarized in Table 1. It is considered that each buffer layer enables similar improvements since comparable V_{oc} and I_{sc} values were obtained in the solar cells inserted with one of the buffer layers. The MoO₃ buffer layer was more effective than the ZnO buffer layer in terms of the FF. I_{sc} was further enhanced, and V_{oc} also increased slightly in the solar cell with both buffer layers. As a result, η_e was enhanced about three times from 0.49% to 1.46% by inserting both MoO₃ and ZnO charge transfer buffer layers.

In order to discuss the interface between the PAT6 and MoO₃ layers, the UV-VIS-NIR absorption spectra of the PAT6 film, MoO₃ film, and PAT6/MoO₃ bi-layer film were measured, and the differential absorption spectrum, which is obtained by subtracting the absorption spectra of the PAT6 and MoO₃ films from that of PAT6/MoO₃ bi-layer film, was investigated, as shown in Figure 5. In these measurements, thinner PAT6 films were prepared compared with the PAT6 layers in the solar cells, the thickness of which was estimated to be 20 nm, in order to clarify weak signals from the interface of PAT6/MoO₃. The absorbance range of 400–600 nm, which is based on the π - π^* transition in PAT6, was decreased, and the absorbance in the near-infrared region appeared upon the formation of the interface of the PAT6 and MoO₃ layers. A similar phenomenon was previously found to be the result of an insulator-metal transition of a CP such as PAT6 upon electrochemical doping [15]. It is noted that the ground-state charge transfer at the interface between the PAT6 and MoO₃ layers occurred to form polarons in the region near the interface. Therefore, it is considered that the conductivity of

PAT6 partially increased near the interface with the MoO₃ layer or the contact resistance was suppressed, resulting in enhancement of the FF.

Figure 4. Current-voltage characteristics of the solar cells with no buffer layer, the MoO₃ buffer layer (6 nm), the ZnO buffer layer (50 nm), and the MoO₃ and ZnO buffer layers (6 nm and 50 nm, respectively) under AM1.5 (100 mW/cm²) solar-illuminated conditions.

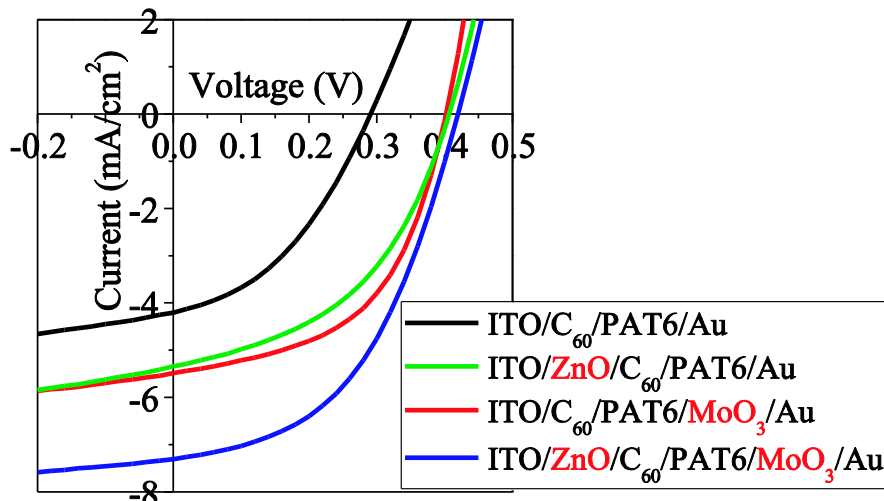
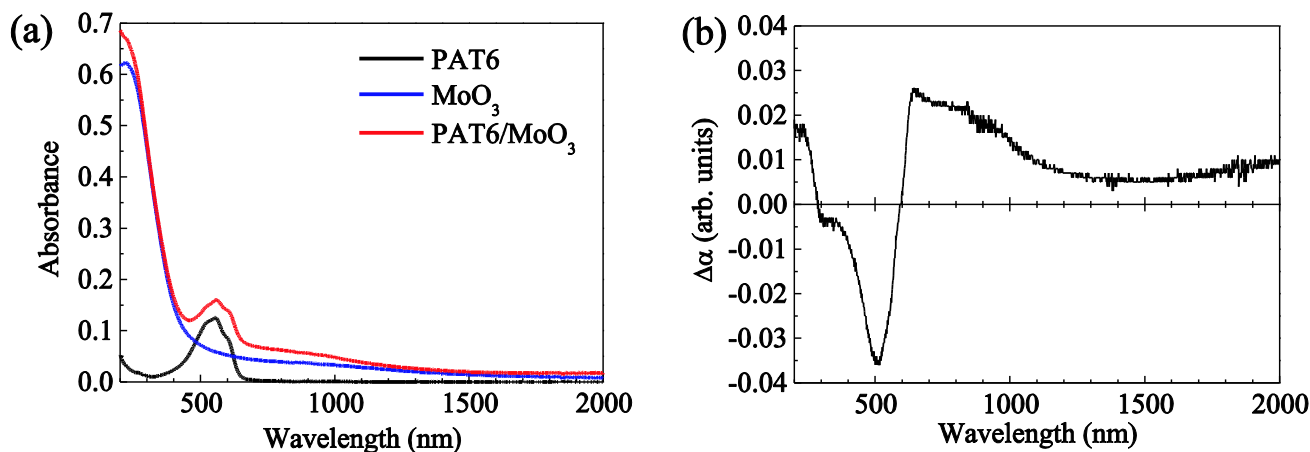


Table 1. Performance parameters in current-voltage characteristics of the solar cells with no buffer layer, ZnO buffer layer (50 nm), MoO₃ buffer layer (6 nm), and ZnO and MoO₃ buffer layers (50 nm and 6 nm, respectively) under solar-illuminated conditions.

Structure of the solar cells	V _{oc} [V]	I _{sc} [mA/cm ²]	Fill Factor	η _e [%]
ITO/C ₆₀ /PAT6/Au	0.29	4.21	0.40	0.49
ITO/ZnO/C ₆₀ /PAT6/Au	0.41	5.35	0.45	0.99
ITO/C ₆₀ /PAT6/MoO ₃ /Au	0.40	5.49	0.52	1.15
ITO/ZnO/C ₆₀ /PAT6/MoO ₃ /Au	0.42	7.31	0.48	1.46

Figure 5. (a) UV-VIS-NIR absorbance spectra of the PAT6 film, MoO₃ film, and PAT6/MoO₃ bi-layer, film and (b) differential absorption spectrum.



Although a similar measurement of the differential absorption spectrum of ZnO/C₆₀ bi-layer films was also carried out, such a marked spectral change was not observed at this stage. From the measurement of the conductivity of the ZnO film, the conductivity under dark and AM1.5 solar-illuminated conditions are found to be 10⁻¹³ S/cm and 10⁻⁸ S/cm, respectively. Since the ZnO film absorbs the UV light included in solar-illumination, and bulk electron traps in ZnO tend to be filled, the marked photoconduction of ZnO could be observed [16,17]. Therefore, it is considered that the efficient electron collection and the suppression of V_{oc} loss by leak current blocking in the solar cell were realized by inserting a 50-nm-thick ZnO buffer layer.

4. Conclusion

Interpenetrating heterojunction organic solar cells with MoO₃ and ZnO charge transport buffer layers were demonstrated. We achieved enhancement of the photovoltaic properties of interpenetrating heterojunction type organic solar cells by inserting a MoO₃ hole buffer layer and a ZnO electron buffer layer. As a result, the EQE of the solar cells exceeded more than 75% and the energy conversion efficiency was improved from 0.49% to 1.46% under AM1.5 solar-illuminated conditions. We discussed the photovoltaic properties in terms of the ground-state charge transfer and reduced the contact resistance at the interface between organic and buffer layers.

Acknowledgements

This work was partly supported by Grants-in-Aid for Scientific Research on Priority Areas, for Young Scientists (A), and for the Japan Society for the Promotion of Science Fellows (No. 225630) from the Ministry of Education, Culture, Sports, Science and Technology, Japan, and by the Global Center of Excellence (Global COE) Program “Center for Electronic Devices Innovation” at Osaka University.

References

1. Morita, S.; Zakhidov, A.A.; Yoshino, K. Doping Effect of Buckminsterfullerene in Conducting Polymer: Change of Absorption Spectrum and Quenching of Luminescence. *Solid State Commun.* **1992**, *82*, 249-252.
2. Sariciftci, N.S.; Smilowitz, L.; Heeger, A.J.; Wudl, F. Photoinduced Electron Transfer from a Conducting Polymer to Buckminsterfullerene. *Science* **1992**, *258*, 1474-1476.
3. Yoshino, K.; Yin, X.H.; Morita, S.; Kawai, T.; Zakhidov, A.A. Enhanced Photoconductivity of C₆₀ Doped Poly(3-alkylthiophene). *Solid State Commun.* **1993**, *85*, 85-88.
4. Sariciftci, N.S.; Braun, D.; Zhang, C.; Srdanov, V.I.; Heeger, A.J.; Wudl, F. Semiconducting polymer-buckminsterfullerene heterojunctions: Diodes, photodiodes, and photovoltaic cells. *Appl. Phys. Lett.* **1993**, *62*, 585-587.
5. Morita, S.; Zakhidov, A.A.; Yoshino, K. Wavelength Dependence of Junction Characteristics of Poly(3-alkylthiophene)/C₆₀ Layer. *Jpn. J. Appl. Phys.* **1993**, *32*, L873-L874.
6. Yu, G.; Pakbaz, K.; Heeger, A.J. Semiconducting polymer diodes: Large size, low cost photodetectors with excellent visible-ultraviolet sensitivity. *Appl. Phys. Lett.* **1994**, *64*, 3422-3424.

7. Yoshino, K.; Tada, K.; Fujii, A.; Conwell, E.M.; Zakhidov, A.A. Novel Photovoltaic Devices Based on Donor-Acceptor Molecular and Conducting Polymer Systems. *IEEE Trans. Electron Devices* **1997**, *44*, 1315-1324.
8. Günes, S.; Neugebauer, H.; Sariciftci, N.S. Conjugated Polymer-Based Organic Solar Cells. *Chem. Rev.* **2007**, *107*, 1324-1338.
9. Umeda, T.; Shirakawa, T.; Fujii, A.; Yoshino, K. Improvement of Characteristics of Organic Photovoltaic Devices Composed of Conducting Polymer-Fullerene Systems by Introduction of ZnO Layer. *Jpn. J. Appl. Phys.* **2003**, *42*, 1475-1477.
10. Shirakawa, T.; Umeda, T.; Hashimoto, Y.; Fujii, A.; Yoshino, K. Effect of ZnO layer on characteristics of conducting polymer/C₆₀ photovoltaic cell. *J. Phys. D: Appl. Phys.* **2004**, *37*, 847-850.
11. Fujii, A.; Shirakawa, T.; Umeda, T.; Mizukami, H.; Hashimoto, Y.; Yoshino, K. Interpenetrating Interface in Organic Photovoltaic Cells with Heterojunction of Poly(3-hexylthiophene) and C₆₀. *Jpn. J. Appl. Phys.* **2004**, *43*, 5573-5576.
12. Kittichungchit, V.; Shibata, T.; Noda, H.; Tanaka, H.; Fujii, A.; Oyabu, N.; Abe, M.; Morita, S.; Ozaki, M. Efficiency Enhancement in Organic Photovoltaic Cell with Interpenetrating Conducting Polymer/C₆₀ Heterojunction Structure by Substrate-Heating Treatment. *Jpn. J. Appl. Phys.* **2008**, *47*, 1094-1097.
13. Hori, T.; Shibata, T.; Kittichungchit, V.; Moritou, H.; Sakai, J.; Kubo, H.; Fujii, A.; Ozaki, M. MoO₃ buffer layer effect on photovoltaic properties of interpenetrating heterojunction type organic solar cells. *Thin Solid Films* **2009**, *518*, 522-525.
14. Ju, X.; Feng, W.; Zhang, X.; Kittichungchit, V.; Hori, T.; Moritou, H.; Fujii, A.; Ozaki, M. Fabrication of organic photovoltaic cells with double-layer ZnO structure. *Sol. Energy Mater. Sol. Cells* **2009**, *93*, 1562-1567.
15. Kaneto, K.; Kohno, Y.; Yoshino, K. Absorption spectra induced by photoexcitation and electrochemical doping in polythiophene. *Solid State Commun.* **1984**, *51*, 267-269.
16. Melnick, D.A. Zinc Oxide Photoconduction, an Oxygen Adsorption Process. *J. Chem. Phys.* **1957**, *26*, 1136-1146.
17. Cordaro, J.F.; Shim, Y.; May, J.E. Bulk electron traps in zinc oxide varistors. *J. Appl. Phys.* **1986**, *60*, 4186-4190.